



An automated optical flow-mediated dilation method for fast screening of endothelial function

Yi Qi^a, Ying Jie Chee^b, Congwen Miao^a, Songhua Zheng^a, Tristan Wen Jie Choo^a,
Ruochong Zhang^a, Quan Wang^d, Michael Yu Qi Zhou^a, Malini Olivo^{a,***}, Rinkoo Dalan^{b,c,**},
Renzhe Bi^{a,*}

^a A*STAR Skin Research Labs (A*STAR SRL), Agency for Science, Technology and Research (A*STAR), 8A Biomedical Grove, #06-06, Immunos 138648, Singapore

^b Tan Tock Seng Hospital (TTSH), 11 Jalan Tan Tock Seng, 308433, Singapore

^c Lee Kong Chian School of Medicine, Nanyang Technological University, 50 Nanyang Avenue, 639798, Singapore

^d Zhuhai UM Science & Technology Research Institute, Zhuhai 519000, China

ARTICLE INFO

Keywords:

Endothelial function
Flow mediated dilation
Diffused speckle pulsatile flowmetry
Blood flow

ABSTRACT

Flow-mediated dilation (FMD) is the non-invasive gold standard for assessing endothelial dysfunction, an early and reversible marker of atherosclerosis, yet its uptake is limited by the cost, complexity, and operator dependence of ultrasound. This study presents an optical method that quantifies endothelial dysfunction using a compact, low-cost, fully automated diffuse speckle pulsatile flowmetry (DSPF) device. The system offers a new Reactive-Hyperemia-Flow-Volume (RHFV) index that achieves a strong correlation ($r = 0.87$) with clinical ultrasound FMD index and high discriminative performance for endothelial dysfunction ($AUC = 0.8475$), demonstrating accuracy comparable to Doppler ultrasound. By enabling convenient, reliable evaluation of endothelial dysfunction at the point of care, this optical technology holds substantial promise as a primary-care screening tool for cardiovascular risk stratification and longitudinal monitoring, with the potential to improve prevention pathways and broaden access to vascular health assessment. Trial registration: NHG DSRB, 2022/00223. Registered 28 April 2022.

1. Introduction

Cardiovascular disease (CVD) remains the leading global cause of mortality, responsible for 17.9 million deaths annually, with atherosclerosis as the underlying cause of stroke, myocardial infarction, and peripheral arterial disease [1–3]. Early detection of atherosclerosis is widely recognized as one of the most effective strategies to mitigate long-term cardiovascular damage. One promising avenue for early screening is the assessment of endothelial dysfunction, which reflects the initial stage of vascular damage [4]. The endothelium plays a vital role in vascular regulation through nitric oxide (NO) signalling [5]. Reduced NO availability leads to a pro-inflammatory and pro-thrombotic phenotype, laying the foundation for atherogenesis [5,6]. Endothelial dysfunction has been identified as a universal marker across all major cardiovascular risk factors and has shown a strong association

with future cardiovascular events [5,7,8]. Conventional endothelial assessment methods have variable limitations. For example, the coronary endothelial function test is invasive, thus unsuitable for large population fast screening. Peripheral tools, such as peripheral arterial tonometry (PAT) and reactive hyperemia Index (RHI), are complementary but less NO-specific, shallow or environment-sensitive, and show variable agreement with conduit-artery function [7].

Flow-mediated dilation (FMD) is an established non-invasive technique used to assess endothelial function by measuring the vasodilation of the brachial artery in response to shear stress during reactive hyperemia [9]. Endothelial dysfunction detected by this method is considered an early event in the development of atherosclerosis [10]. FMD has been shown to correlate with coronary endothelial function, as well as with the severity and extent of coronary atherosclerosis, making it a surrogate marker for vascular health [11]. Additionally, FMD is reversible with

* Co-corresponding author.

** Co-corresponding author.

*** Co-corresponding author.

E-mail address: bi_renzhe@asrl.a-star.edu.sg (R. Bi).

risk factor modification, making it a compelling and therapeutic marker of response [12,13]. However, FMD has several limitations: ultrasound systems are expensive, the technique is operator-dependent and requires rigorous training, and inter-operator variability can be substantial [14]. New users typically need 6 weeks of hands-on training to achieve acceptable reproducibility, and measurements remain time-consuming with notable inter-operator variability [15]. These challenges restrict its application outside of specialized clinical environments, limiting its accessibility in primary care and large-scale community screening programs.

In recent years, many advances have been made in noninvasive vascular assessment based on optical technology. Various optical methods, such as diffuse correlation spectroscopy (DCS) [16], laser speckle contrast imaging (LSCI) [17], and photoacoustic imaging (PAI) [18], have a wide range of applications in both pre-clinical and medical research fields. However, some challenges limit the clinical application of these techniques in endothelial function assessment, for example, DCS typically requires high-power lasers and high sensitivity single photon counting detectors, LSCI is limited by shallow penetration depth (<1mm), while PAI requires expensive instruments and high power pulsed lasers. Diffuse Speckle Pulsatile Flowmetry (DSPF), also known as diffuse speckle contrast analysis (DSCA), is an emerging optical technique for blood flow assessment [19,20]. Based on the analysis of laser speckle patterns formed by the diffused light scattered by the tissue in vivo, DSPF evaluates blood flow rate and tissue perfusion non-invasively [21–23]. It offers a high measurement frequency of > 300 Hz, deep tissue penetration (1 – 20 mm), and a simpler, more cost-effective system architecture [24,25]. DSPF has demonstrated significant potential in hemodynamic monitoring and the early diagnosis of peripheral artery disease [26]. Similar technologies like speckle contrast optical spectroscopy (SCOS) and diffuse speckle contrast flowmeter (DSCF) have been reported to monitor blood flow in the brain, muscles, and tumor tissues, assisting in the diagnosis and treatment of the relevant medical conditions [27–34]. However, most of the reported diffuse laser speckle devices still rely on a PC or laptop for system control and user interfacing, which limit their portability, increase the wiring complexity and restrict deployment in clinical settings. Based on our knowledge, a fully integrated single-unit DSPF for FMD-aligned testing has not been reported.

In this paper, we present, to our knowledge, the first-in-class fully integrated, self-contained, and compact standalone DSPF system based on a single board computer (SBC) for simultaneous monitoring of blood flow and volume. All data acquisition, processing, and display functions are integrated into a single compact unit, eliminating the need for external computing or auxiliary hardware. Moreover, a new measurement protocol has been validated for the FMD assessment through a clinical study with a novel biomarker, Reactive-Hyperemia-Flow-Volume (RHFV) index, which is derived from synchronized blood flow index (BFI) and blood volume index (BVI) signals. This marker was validated against the current gold standard FMD measurement for assessing endothelial function. Our findings demonstrate a strong correlation between the RHFV index and traditional Doppler FMD measurements, with comparable diagnostic performance in distinguishing subjects with and without endothelial dysfunction.

2. Materials and methods

2.1. Instrument design

Diffuse speckle pulsatile flowmetry (DSPF) is a non-invasive optical technique for measuring blood flow in deep tissues. The fundamental principle involves illuminating biological tissue with a coherent light source, such as a laser, and extracting blood flow information from the speckle pattern formed by scattered light. The fluctuations in speckle intensity reflect the movement characteristics of red blood cells within the tissue. The speckle contrast (K) quantifies these fluctuations by

calculating the ratio of the standard deviation (σ) of intensity to the mean intensity (I). Where the equation is [35]:

$$K = \frac{\sigma}{I}$$

The essence of DSPF lies in leveraging the relationship between speckle contrast and the normalized electric field autocorrelation function, from which the Blood Flow Index (BFI) can be derived [24]:

$$BFI = \frac{1}{K^2} = \frac{I^2}{\sigma^2}$$

Moreover, the device can measure blood volume through laser absorption, yielding a Blood Volume Index (BVI). BVI is defined as the inverse of the mean detected intensity at 785 nm because hemoglobin absorption increases with blood volume. Under a fixed geometry, increases in local blood volume reduce detected intensity via the Beer-Lambert relationship. Consequently, the BVI can be estimated by calculating the inverse of the mean intensity (I) received at the detection end [24]:

$$BVI = \frac{1}{I}$$

Here, we present a fully integrated, compact, and cost-effective DSPF system capable of high-frame-rate measurement of both blood flow and blood volume for FMD testing. Fig. 1(a) shows the instrument architecture housed in a 25 × 15 × 14 cm, ~1 kg chassis comparable to a clinical blood-pressure unit. Subsystems include a 785 nm low-noise laser module, precision multimode-fiber fixtures that butt-couple to the sensor for stable channel geometry, and a high-speed CMOS. An embedded SBC with a touchscreen replaces an external PC and executes the entire workflow, system control, real-time acquisition, processing, and display, within the instrument. The controller orchestrates laser drivers and temperature regulation, schedules closed-loop control of the laser module, and streams camera data (USB3/DMA) at high frame rates. On-device algorithms perform background flattening, ROI mapping, speckle-contrast computation, cycle-peak detection, and motion/quality control (including lightweight AI denoising), rendering results instantly on the touchscreen. The system logs raw and processed data, supports secure export (e.g., USB/Wi-Fi), and provides calibration, firmware update, and audit utilities, delivering a self-contained, clinic-ready platform without any external computer.

Probe engineering prioritizes contact stability and clinical workflow. As shown in Fig. 1(b), the multi-purpose arm probe integrates two multimode fibers in a rotatable fixture, preserving fiber tips spacing while allowing angular alignment to the radial artery. Attachment is via elastic band for rapid screening or disposable adhesive patch for longer sessions. The probe is 3D-printable, supporting low-cost, reproducible manufacturing. In this study it was deployed on the radial artery at the wrist, enabling hands-free, gel-free measurements with robust speckle dynamics throughout cuff occlusion and reperfusion periods.

2.2. Clinical validation protocol

The validation study was conducted in Tan Tock Seng Hospital (TTSH) in Singapore (DSRB approval reference 2022/00223). We recruited 20 healthy volunteers with normal endothelial function and 20 individuals with diabetes. Simultaneous data collection was performed with the new DSPF device and longitudinal B-mode images of the brachial artery with concurrent Doppler pulse wave velocity were captured using ultrasound (Terason™). To enable simultaneous acquisition and preserve the ultrasound gold-standard protocol, the Doppler probe was positioned on the proximal radial artery (forearm) according to clinical FMD practice, while the optical DSPF probe was secured over the radial artery at the wrist, downstream of the upper-arm occlusion cuff, as shown in Fig. 2(a). This configuration prevented physical interference between probes and eliminated temporal/environmental

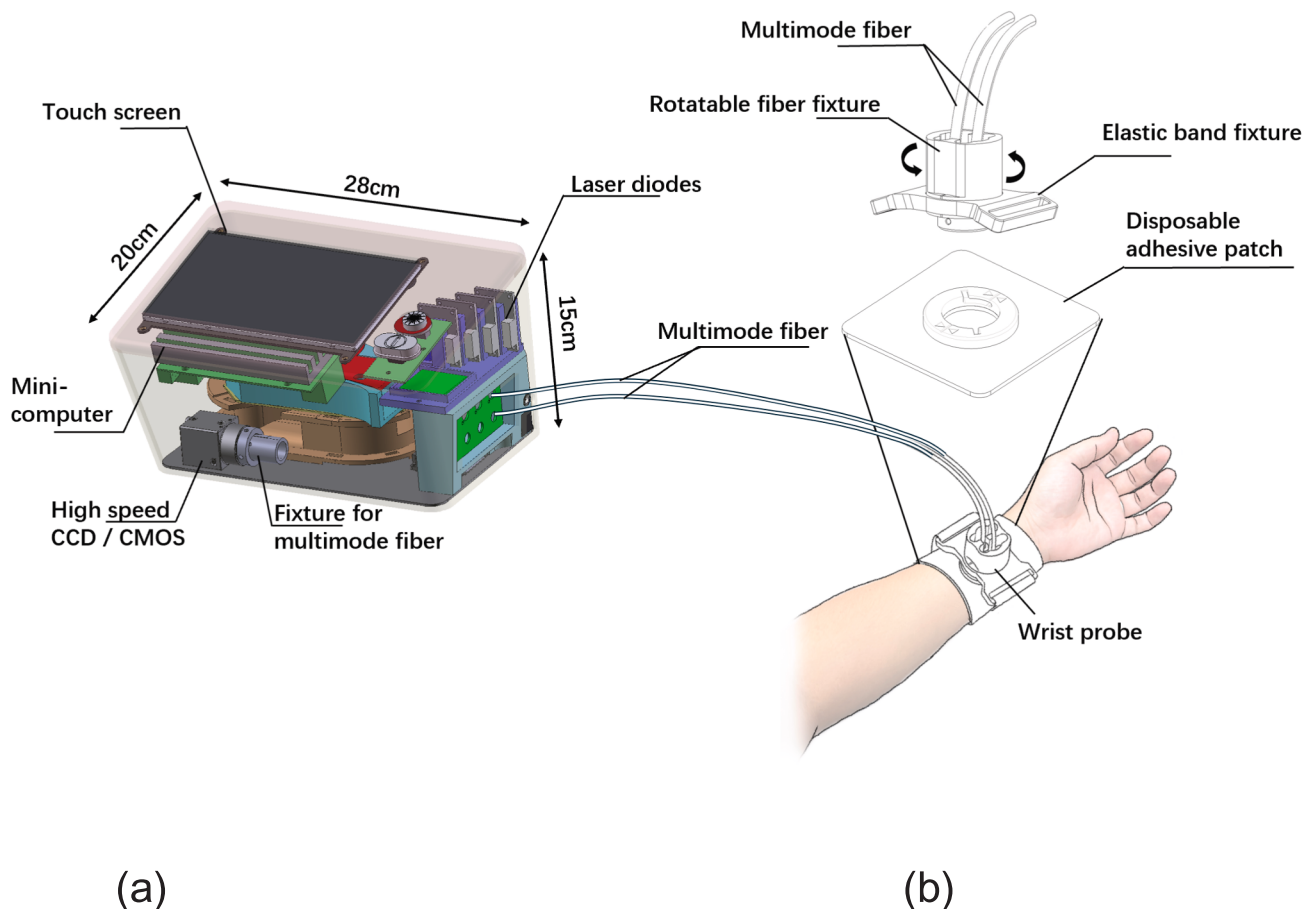


Fig. 1. (a) the schematic of the compact DSPF system, and (b) the multi-purpose probe design for the radial artery blood flow measurement.

confounders across modalities. The validation protocol is aligned with the FMD procedure performed by a trained operator adhering to consensus guidelines at room temperature (22–24 °C) [9]. With the participant in supine position, arm at heart level with elbow supported, a blood pressure cuff was placed on the participant's left forearm below the olecranon process, and a DSPF wearable probe was secured to the subject's wrist using an elastic strap to measure blood flow signals in the radial artery. We adhered to the three phases of the standard FMD measurement:

- (i) Baseline: simultaneous measurement of blood flow and blood volume by DSPF device for 1 min in the relaxed state. The baseline diameter of the brachial artery was measured by Doppler Ultrasound for 1 min;
- (ii) Occlusion: The compression cuff was inflated to 200 mmHg to occlude blood flow in the brachial artery for 5 min;
- (iii) Reperfusion: simultaneous measurement of blood flow, blood volume by DSPF device and continuous imaging of the brachial artery by Doppler ultrasound for 3 min.

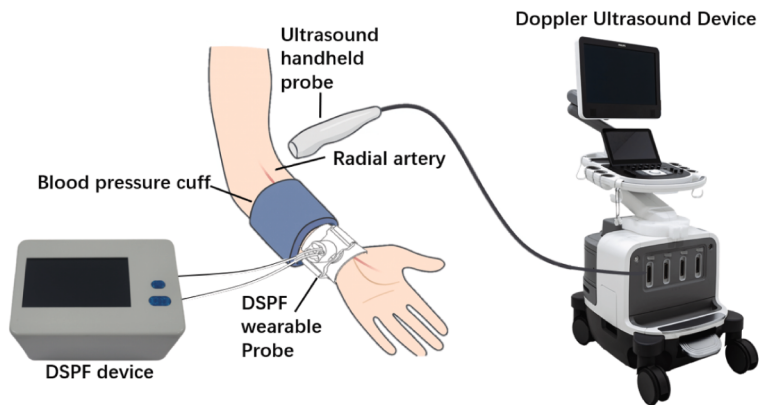
Before processing the collected data, it will undergo preliminary screening according to the following criteria to ensure the quality of experimental data: 1) During the experiment, the subject's tested arm exhibited no motion or other body movement. 2) The signal-to-noise ratio of the test results for the ultrasound device and DSPF device remained stable and consistent throughout the entire testing process. 3) No abnormal signals (sudden drops or spikes in data) were observed in the experimental results. FMD analysis was performed using an edge detection software (Bloodflow Analyzer, Reeds Electronics) to track the brachial artery diameter accurately. FMD was calculated by taking the

difference between peak and baseline brachial artery diameter $\times 100\%$. The blood flow and blood volume data were used to calculate the DSPF device index with the specific algorithm.

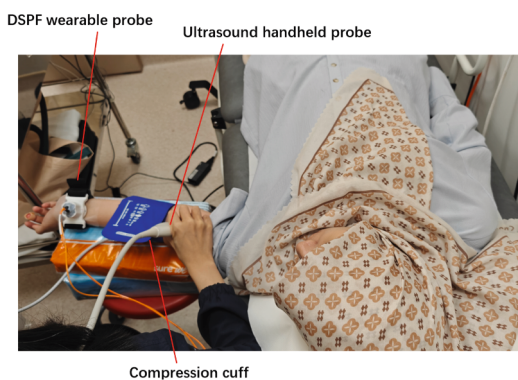
2.3. Data processing algorithms

Local vasodilation during reactive hyperemia is driven by shear stress, which increases with blood speed. While Doppler ultrasound infers shear by measuring peak flow velocity, DSPF directly quantifies red blood cell motion through rapid speckle-contrast fluctuations, and red blood cell volume through the light absorption, thus producing the Blood Flow Index (BFI) and the Blood Volume Index (BVI) [25]. Because vasodilation reflects the vessel's response to elevated shear and flow, BFI and BVI can capture the same physiological stimulus that underlies diameter changes in FMD testing. Therefore, in contrast to Doppler ultrasound devices which assess endothelial dysfunction during FMD testing by directly measuring changes in vessel diameter before and after occlusion, DSPF device offers an alternative approach by simultaneously measuring both BFI and BVI. To evaluate whether DSPF device can evaluate endothelial function comparable to Doppler ultrasound, we have conducted a Flow-Mediated Dilation (FMD) test using the radial artery at the crook of the arm using probes from both DSPF device and a Doppler ultrasound device (DUD) simultaneously. The acquisition of FMD data from DUD is well known as the edge-detection method, while the DSPF device measures the BFI and BVI signal directly. As shown in Fig. 3(a), compared to the baseline phase, the vessel diameter increased during the reperfusion phase, and the BFI also showed an elevation during reperfusion.

Fig. 3(a) shows a set of raw BFI data (the occlusion phase was omitted due to no useful information) for the FMD testing that was



(a)



(b)

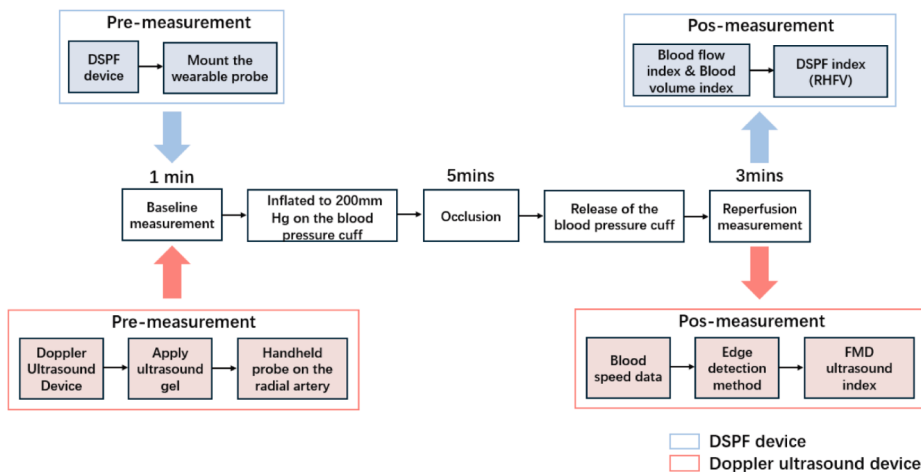
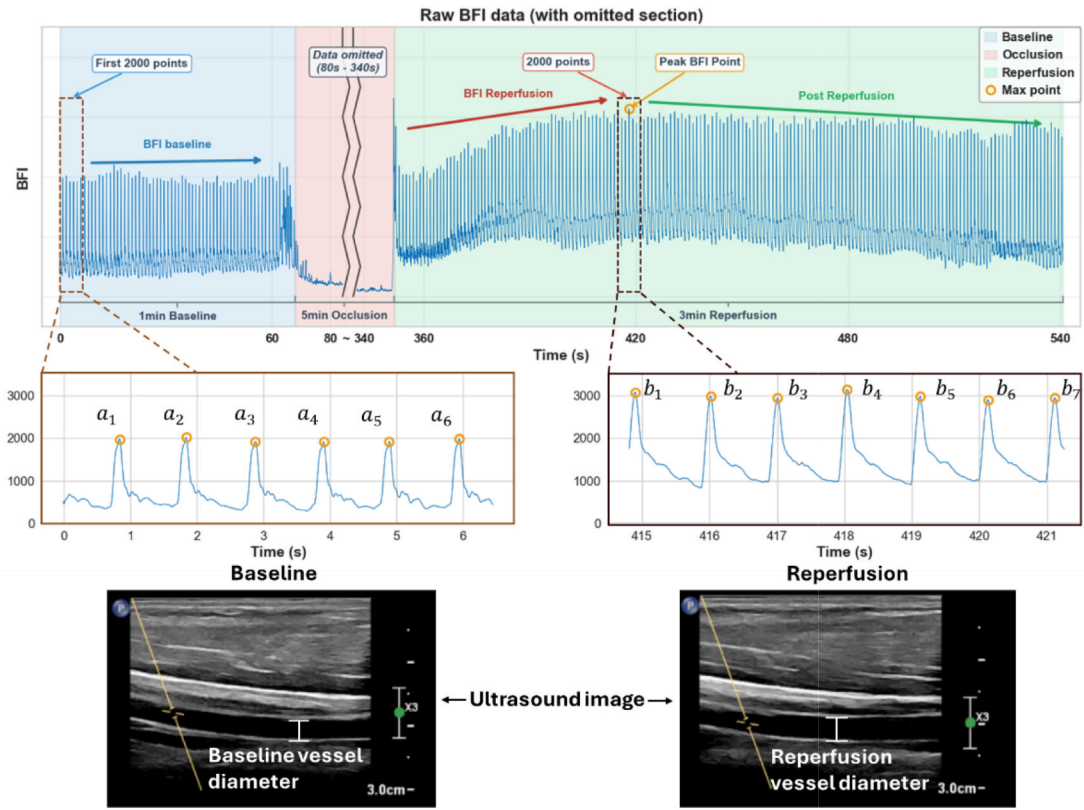


Fig. 2. (a) The clinical trial set up and time sequence for baseline, occlusion, and reperfusion phase, (b) a photo of the clinical trial, and (c) the workflow of the DSPF device and the DUD device for the FMD assessment.

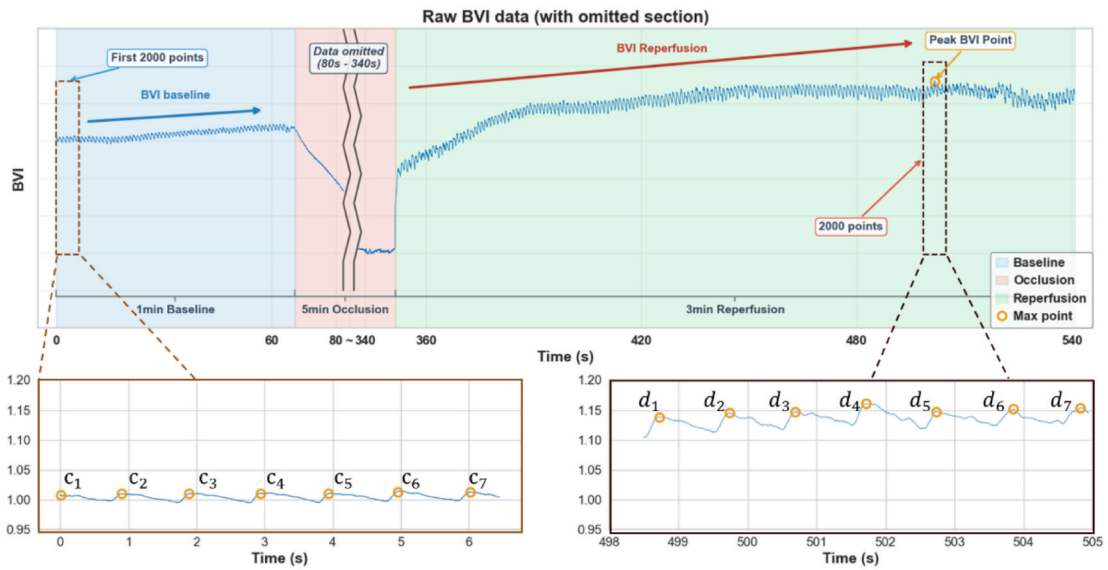
acquired from DSPF device. We selected 2,000 data points each from the baseline and reperfusion phases. The baseline data were sampled from the start of the measurement, while the reperfusion data were centered on the point of maximum value within that phase. Then, as illustrated in Fig. 3(b), we extract the BVI data with same method. Due to blood flow is pulsatile and periodic, we extracted the peak points from each cycle

among those 2,000 points that serve as a noise-reduction filter, and then calculated the average value of these peak points to obtain four features from BFI and BVI data:

$$BFI_{Baseline} = \left(\sum_{i=1}^n a_i \right) / n$$



(a)



(b)

Fig. 3. (a) raw BFI and data of one run of FMD data acquisition from DSPF device and the selected data to calculate key features: $BFI_{Baseline}$, $BFI_{MaxReperfusion}$, with the comparison between the BFI data and the ultrasound image in the baseline and reperfusion phase, (b) raw BVI data of one run of FMD data acquisition from DSPF device and the selected data to calculate key features: $BVI_{Baseline}$, and $BVI_{MaxReperfusion}$, (c) the time delay between $BFI_{MaxReperfusion}$ and $BVI_{MaxReperfusion}$ among healthy subject and patient.

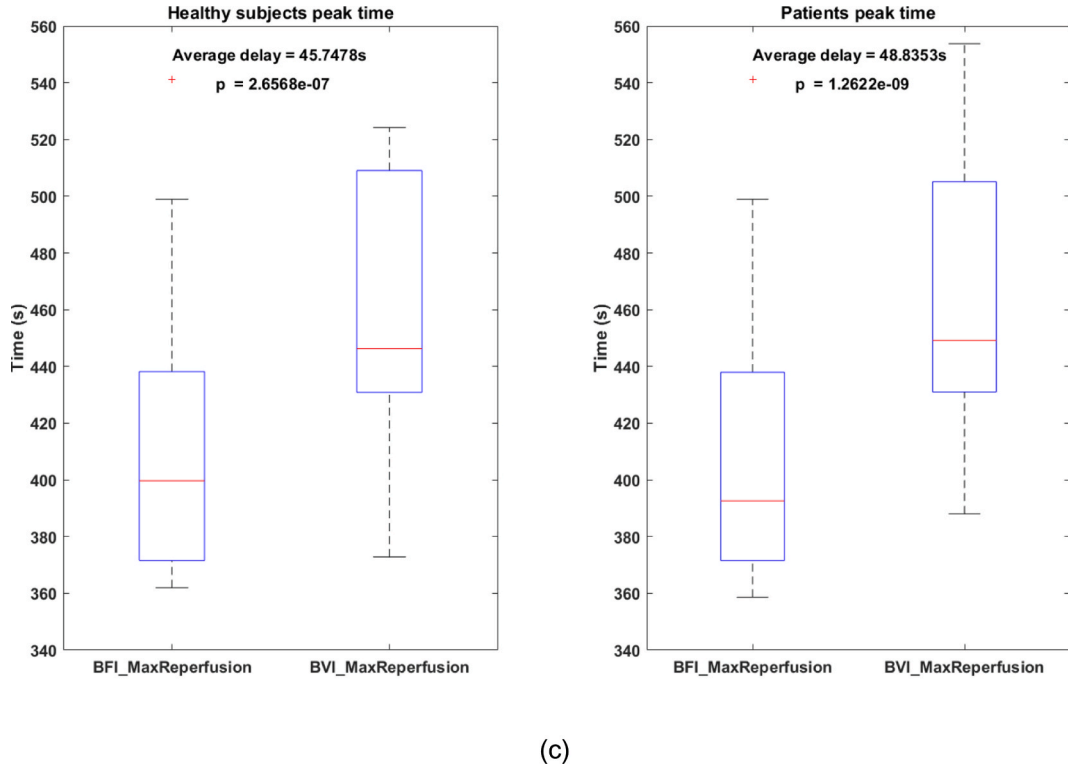


Fig. 3. (continued).

$$BFI_{MaxReperfusion} = \left(\sum_{i=1}^n b_i \right) / n$$

$$BVI_{Baseline} = \left(\sum_{i=1}^n c_i \right) / n$$

$$BVI_{MaxReperfusion} = \left(\sum_{i=1}^n d_i \right) / n$$

The system acquires blood-flow (BFI) and blood-volume (BVI) signals simultaneously from the same field of view and clock, yielding intrinsic temporal co-registration. During the reperfusion phase, the analysis windows for BFI and BVI are anchored to their own peak times rather than a common marker. During the clinical trial, we consistently observe a short lag of the BVI peak after the BFI peak. As shown in Fig. 3(c), BVI peaks average delayed $\Delta t = 45.7478$ s after BFI peaks among healthy subject group ($p = 2.6568 \times 10^{-7}$), while patient group has delayed $\Delta t = 48.8353$ s ($p = 1.2622 \times 10^{-9}$). This timing offset is physiologically plausible given the measurement geometry: signals are acquired at the radial artery on the wrist while occlusion is applied at the upper arm. After cuff release, the velocity surge propagates distally and is detected by BFI almost immediately, whereas the volume response captured by BVI reflects slower processes: the artery and smaller downstream vessels gradually dilate, the pressure across the vessel wall settles back to normal, and more capillaries open and fill. These slower processes make the BVI reach its maximum after BFI. Therefore, we introduce the Reactive-Hyperemia-Flow-Volume (RHFV) index, which is calculated by above four features:

$$RHFV = BFI^{BVI} = \left(\frac{BFI_{MaxReperfusion}}{BFI_{Baseline}} \right)^{\left(\frac{BVI_{MaxReperfusion}}{BVI_{Baseline}} \right)}$$

Here, BFI is a surrogate of red blood cell motion speed (shear), and BVI is a surrogate of local blood volume (absorption). Because reperfusion exhibits an early velocity surge followed by slower volume expansion,

$BFI_{MaxReperfusion}$ and $BVI_{MaxReperfusion}$ are identified at their own peaks in the reperfusion phase, baselines are computed from the initial resting segment. In log form,

$$\text{Log}(RHFV) = BVI \cdot \text{Log}(BFI) = \left(\frac{BVI_{MaxReperfusion}}{BVI_{Baseline}} \right) \cdot \text{Log} \left(\frac{BFI_{MaxReperfusion}}{BFI_{Baseline}} \right)$$

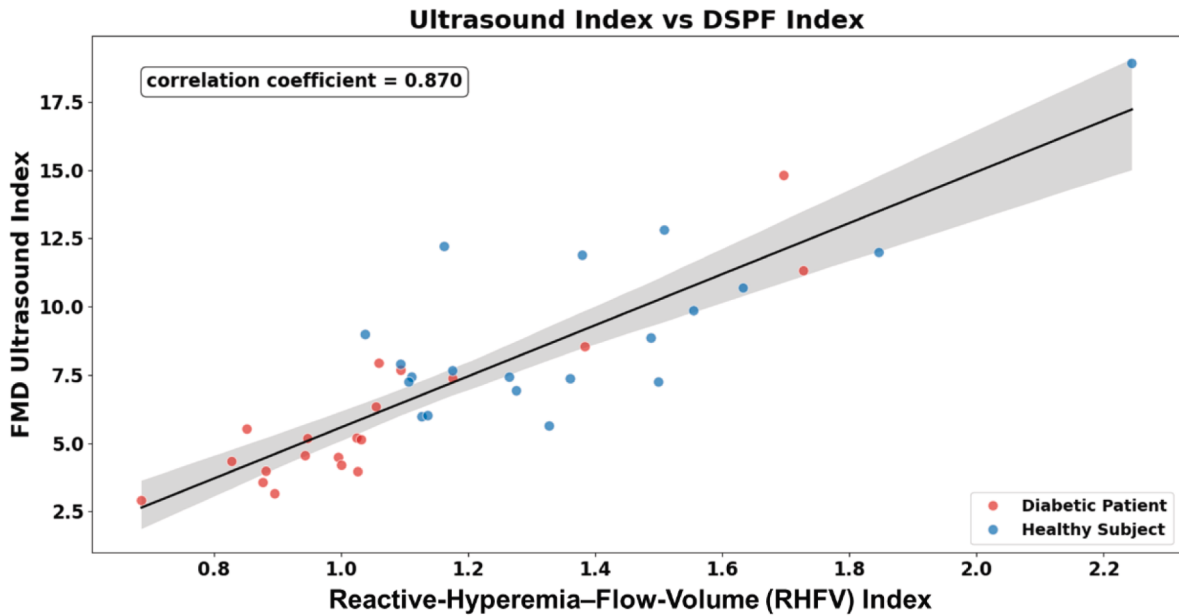
showing that volume response weights the shear-linked velocity response, implementing a physiologic “AND” condition that rises chiefly when both components are present. This enhances specificity to shear-mediated vasoreactivity while mitigating scaling differences.

With the proposed RHFV, our DSPF platform can achieve a non-invasive, fully automated workflow for endothelial function FMD assessment. In contrast to Doppler ultrasound based FMD, the method requires no handheld transducer, gel, or operator-dependent caliper measurements, the closed-loop cuff inflation/deflation and real-time analysis at 330 Hz produce a single RHFV within minutes. By preserving pulsatility, supporting multi-site probes, and standardizing acquisition and analysis on device, this approach improves reproducibility and scalability while retaining the physiological specificity of shear-mediated vasodilation, constituting a substantive methodological advance over traditional FMD testing.

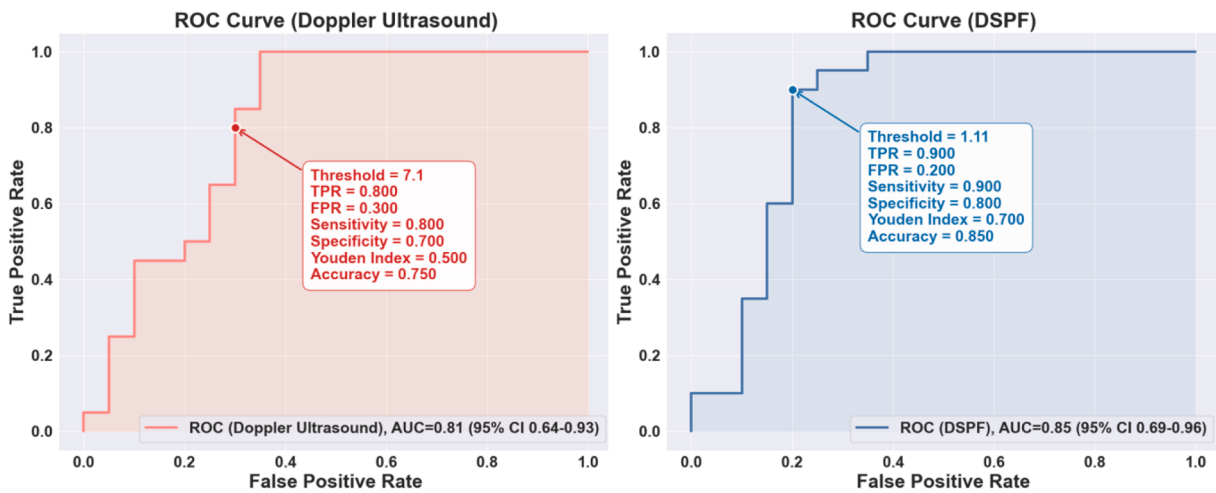
3. Results and analysis

We analyzed two datasets from 40 participants, including 20 patients with diabetes and 20 healthy individuals. Each subject underwent flow-mediated dilation (FMD) testing with a Doppler ultrasound device and with the DSPF device.

Fig. 4(a) shows the cross-method correlation between the DSPF-derived RHFV index and the Doppler-derived FMD index (FMD_{DUD}), which demonstrates a strong linear relationship between the two modalities across the full index range (patients in red, healthy in blue), with correlation coefficient is $r = 0.870$. This correlation is highly significant ($t \approx 10.88$; two-sided $p \ll 0.001$) and the approximate 95% confidence interval for correlation coefficient by Fisher's z-transform is 0.77–0.93.



(a)



(b)

Fig. 4. (a) The correlation between FMD_{DUD} index and RHFV index, while correlation ratio $r = 0.87$, (b) the ROC curve of DUD and DSPF method to distinguish the patients and healthy subjects, while the FMD_{DUD} has 0.8 sensitivity and 0.7 specificity, the DSPF index (RHFV) has 0.9 sensitivity and 0.8 specificity.

The regression band indicates good agreement over the dynamic range, including higher DSPF values where ultrasound indices are likewise elevated, with no single outlier dominating the fit.

To evaluate the overall diagnostic performance of DSPF device compared to the Doppler ultrasound in FMD-based endothelial dysfunction assessment, we plotted the receiver operating characteristic (ROC) curves, as shown in Fig. 4(b), we report area under the curve (AUC), optimal operating points highlighted in the plots (threshold, sensitivity, specificity), Youden’s index, and accuracy. Under the same testing conditions, the Doppler ultrasound ROC achieved an AUC of 0.81 (95% CI 0.64–0.93). At the displayed threshold of 7.1, the true-positive rate (TPR) was 0.80 and the false-positive rate (FPR) 0.30, yielding sensitivity = 0.80, specificity = 0.70, Youden’s index = 0.50, and

accuracy = 0.75. The DSPF ROC achieved a higher AUC of 0.85 (95% CI 0.69–0.96). At the displayed threshold of 1.11, TPR = 0.90 and FPR = 0.20, corresponding to sensitivity = 0.90, specificity = 0.80, Youden’s index = 0.70, and accuracy = 0.85.

Both evaluation methods demonstrate a statistically significant difference between the healthy group and the diabetes group, indicating that vascular health is markedly reduced in diabetes patients compared to healthy individuals. The correlation and ROC analyses support both the discriminative and convergent validity of the DSPF device for endothelial dysfunction screening. First, DSPF’s AUC (0.85) is comparable to, and numerically exceeds, Doppler ultrasound’s AUC (0.81), with overlapping confidence intervals, indicating similar overall diagnostic accuracy in this cohort. At the indicated operating point, DSPF

provides a more favorable trade-off, translating into better balanced classification and higher accuracy. Second, the strong cross-method correlation shows that DSPF's continuous index tracks the physiological changes captured by ultrasound FMD, supporting use of DSPF as a quantitative surrogate in settings where ultrasound is impractical. Clinically, higher sensitivity at a reasonable specificity suggests DSPF can serve as an effective front-line, portable screen to flag individuals for confirmatory testing or intervention, particularly in primary-care and community environments. The tight correlation further implies DSPF may be suitable for longitudinal monitoring of endothelial function, therapy response, or disease progression.

4. Discussion

This work introduces a fully integrated, multi-channel DSPF platform, a new optical FMD measurement protocol, and an accompanying analysis pipeline that together deliver real-time, operator-independent assessment of endothelial function. The clinical validation protocol was intentionally aligned with ultrasound FMD to enable head-to-head comparison while exploiting the strengths of optics. Cuff occlusion/release followed standard timings while the optical probe was secured on the wrist to stabilize measurement during inflation/deflation. The high frame rate (330 Hz) acquisition captured the fast transients that are typically blurred by temporal averaging in single mode fiber based DSPF systems. Importantly, the DSPF index is computed from peak-of-cycle features in predefined baseline and reperfusion windows, preserving physiological timing and reducing susceptibility to baseline drift.

Validation study results provide convergent and discriminative validity. Across 40 participants, the RHFV index correlated strongly with the Doppler FMD index, indicating that continuous optical metrics track the same vascular responsiveness captured by ultrasound diameter change. We emphasize that DSPF index (RHFV) does not measure conduit artery diameter. Rather, it is a reactive-hyperemia-derived optical surrogate that reflects the hemodynamic consequences (blood flow and volume changes) of upstream vasodilation in distal vessels. This functional index correlates with ultrasound FMD in our cohort, supporting its use as a surrogate readout for endothelial responsiveness in contexts where ultrasound is impractical. In classification analyses, DSPF achieved higher sensitivity and specificity than the DUD. These findings support DSPF as both a quantitative surrogate for ultrasound FMD and a practical front-line screen in settings where ultrasound is unavailable or impractical. The strong cross-method agreement further suggests suitability for longitudinal monitoring of endothelial recovery or decline under lifestyle or pharmacologic interventions.

From a technological standpoint, the platform advances the field by linking optical hardware constraints to physiological interpretability. Multimode collection increases photon throughput, allowing low laser power (<5 mW per channel) while sustaining high SNR, and the fixed fiber-to-sensor registration stabilizes the measurement kernel across sessions. At the same time, dual-signal (BFI/BVI) acquisition adds redundancy: when motion or illumination changes perturb one channel, the other can serve as a timing or plausibility check. Embedding denoising, artifact rejection, and index computation on device standardizes analysis across sites and operators—an essential step toward multi-center reproducibility, regulatory clearance, and real-world deployment.

The translational implications are substantial. Because the device is portable, low-power, and hands-free, it can be deployed in primary care, community screening, and rehabilitation settings to identify endothelial dysfunction before structural atherosclerosis is overt. Beyond diabetes risk stratification, the same protocol can be adapted to evaluate peripheral arterial disease, microvascular angina/HFpEF, hypertension and vascular aging, and perioperative or critical-care states where microcirculatory adequacy is prognostically important. By reducing cost and operator dependence while preserving physiological specificity to shear-mediated vasodilation, DSPF has the potential to shift endothelial

testing from specialist labs to point-of-care pathways, with expected downstream benefits in prevention, triage, and outcome tracking.

5. Conclusion

This study presents a novel, fully-integrated, compact, and portable DSPF system for non-invasive assessment of endothelial function. The optical FMD approach is operator-independent and gel-free, with a wearable probe and on-device acquisition/processing that standardize measurements and reduce inter-operator variability. Our findings demonstrate that the proposed portable DSPF device delivers endothelial-function assessments equivalent in accuracy to Doppler ultrasound. The proposed DSPF system offers several key advantages over traditional Doppler ultrasound-based methods, including affordability, portability, and multi-channel capability. Through the introduction of a new optical-based, reactive hyperemia flow and volume index, the RHFV, we demonstrated a strong correlation ($r = 0.87$) against the clinical gold standard, FMD measurements via Doppler ultrasound device, while the proposed DSPF device has comparable diagnostic performance in distinguishing subjects with and without endothelial dysfunction ($AUC = 0.85$). Because optical probe samples the wrist radial artery, local responses may include contributions from microvascular perfusion and downstream hemodynamics in addition to conduit artery behavior, accordingly, we avoid claiming direct diameter measurement and frame RHFV index as a physiologically coupled surrogate.

This research paves the way for the development of a scalable and user-friendly tool for vascular health screening in decentralized and resource-limited healthcare environments, particularly in the context of diabetes and other cardiovascular risk factors. Further studies are warranted to explore the potential of this technology in broader clinical applications, including the assessment of coronary microvascular dysfunction, peripheral arterial disease, hypertension, and vascular aging.

CRedit authorship contribution statement

Yi Qi: Writing – review & editing, Writing – original draft, Validation, Software, Investigation, Formal analysis, Data curation. **Ying Jie Chee:** Writing – review & editing, Validation, Methodology, Investigation, Data curation. **Congwen Miao:** Writing – review & editing, Formal analysis. **Songhua Zheng:** Writing – review & editing. **Tristan Wen Jie Choo:** Writing – review & editing. **Ruochong Zhang:** Writing – review & editing. **Quan Wang:** Writing – review & editing. **Michael Yu Qi Zhou:** Writing – review & editing, Formal analysis. **Malini Olivo:** Supervision, Investigation, Funding acquisition, Conceptualization. **Rinkoo Dalan:** Writing – review & editing, Supervision, Funding acquisition, Conceptualization. **Renzhe Bi:** Writing – review & editing, Supervision, Resources, Project administration, Investigation, Funding acquisition, Formal analysis, Conceptualization.

Declaration of competing interest

The authors declare that they have no known competing financial interests or personal relationships that could have appeared to influence the work reported in this paper.

Acknowledgement

This work was supported by the Agency for Science, Technology and Research (A * STAR), Singapore, through BMRC CRF fund 2024, IAF-pp fund H24J4a0146, NMRC OF-IRG project OFIRG25jan-0092. We thank James Dyson Foundation and Ng Teng Fong Foundation for their support to Tan Tock Seng Hospital (Dalan R & Chee YJ), Personalized Cardiometabolic Risk Management Program.

Data availability

Data will be made available on request.

References

- [1] C.-H. Sia, et al., Atherosclerotic cardiovascular disease landscape in Singapore, *Front. Cardiovasc. Med.* 11–2024 (2024).
- [2] H. Ueshima, et al., Cardiovascular Disease and Risk Factors in Asia, *Circulation* 118 (25) (2008) 2702–2709.
- [3] J.-E. Tarride, et al., A review of the cost of cardiovascular disease, *Can. J. Cardiol.* 25 (6) (2009) e195–e202.
- [4] P. Poredoš, M. Kaja Jezovnik, Markers of preclinical atherosclerosis and their clinical relevance, *Vasa* 44 (4) (2015) 247–256.
- [5] G. Giannotti, U. Landmesser, Endothelial dysfunction as an early sign of atherosclerosis, *Herz* 32 (7) (2007) 568–572.
- [6] A. Knutsson, H. Bøggild, Shiftwork and Cardiovascular Disease: review of Disease Mechanisms, *Rev. Environ. Health* 15 (4) (2000) 359–372.
- [7] S. Giannitsi, et al., Endothelial dysfunction and heart failure: a review of the existing bibliography with emphasis on flow mediated dilation, *JRSM Cardiovasc. Dis.* 8 (2019) 2048004019843047.
- [8] T. Maruhashi, et al., Endothelial dysfunction, increased arterial stiffness, and cardiovascular risk prediction in patients with coronary artery disease: FMD-J (flow-mediated dilation Japan), *Study a. J Am Heart Assoc* 7 (14) (2018).
- [9] D.H.J. Thijssen, et al., Expert consensus and evidence-based recommendations for the assessment of flow-mediated dilation in humans, *Eur. Heart J.* 40 (30) (2019) 2534–2547.
- [10] H. Korkmaz, O. Onalan, Evaluation of endothelial dysfunction: flow-mediated dilation, *Endothelium* 15 (4) (2008) 157–163.
- [11] J.T. Kuvin, et al., Peripheral vascular endothelial function testing as a noninvasive indicator of coronary artery disease, *JACC* 38 (7) (2001) 1843–1849.
- [12] R.A. Vogel, Measurement of endothelial function by brachial artery flow-mediated vasodilation, *Am. J. Cardiol.* 88 (2, Supplement 1) (2001) 31–34.
- [13] R. Dalan, et al., Proof-of-concept study for an enhanced surrogate marker of endothelial function in diabetes, *Sci. Rep.* 8 (1) (2018) 8649.
- [14] M.D. Faulx, A.T. Wright, B.D. Hoyt, Detection of endothelial dysfunction with brachial artery ultrasound scanning, *Am. Heart J.* 145 (6) (2003) 943–951.
- [15] A.S. Dhar, et al., Flow-mediated dilatation: learning curve study with a novice operator, *Artery Res.* 30 (1) (2024) 13.
- [16] S.A. Carp, M.B. Robinson, M.A. Franceschini, Diffuse correlation spectroscopy: current status and future outlook, *Neurophotonics* 10 (1) (2023) 013509.
- [17] D.A. Boas, A.K. Dunn, Laser speckle contrast imaging in biomedical optics, *J. Biomed. Opt.* 15 (1) (2010), pp. 011109–011109-12.
- [18] J. Park, et al., Clinical translation of photoacoustic imaging, *Nat. Rev. Bioeng.* 3 (3) (2025) 193–212.
- [19] J. Hong, et al., Non-ergodicity and noise-corrected diffuse speckle contrast analysis in deep tissue blood flow measurement, *Biomed. Opt. Express* 16 (5) (2025) 1856–1870.
- [20] H. Jung, et al., Machine-learning-based diabetes classification method using blood flow oscillations and Pearson correlation analysis of feature importance, *Mach. Learn.: Sci. Technol.* 5 (4) (2024).
- [21] B. Liu, et al., Mapping of blood flow and slow speckle tissue dynamics using laser speckle contrast imaging, *Biomed. Opt. Express* 16 (9) (2025) 3712–3724.
- [22] H.L. Liu, et al., Wide dynamic range measurement of blood flow *in vivo* using laser speckle contrast imaging, *J. Biomed. Opt.* 29 (1) (2024) 016009.
- [23] L. Kobayashi Frisk, et al., Comprehensive workflow and its validation for simulating diffuse speckle statistics for optical blood flow measurements, *Biomed. Opt. Express* 15 (2) (2024) 875–899.
- [24] R. Bi, J. Dong, K. Lee, Multi-channel deep tissue flowmetry based on temporal diffuse speckle contrast analysis, *Opt. Express* 21 (19) (2013) 22854–22861.
- [25] R. Bi, et al., Fast pulsatile blood flow measurement in deep tissue through a multimode detection fiber, *J. Biomed. Opt.* 25 (5) (2020) 055003.
- [26] R. Bi, et al., A portable optical pulsatile flowmetry demonstrates strong clinical relevance for diabetic foot perfusion assessment, *APL Bioeng.* 8 (1) (2024) 016109.
- [27] M.-C. Hsieh, et al., Improving the early diagnosis and clinical outcomes of shock patients via laser speckle contrast imaging assessment of peripheral hemodynamics, *iScience* 27 (12) (2024).
- [28] A. Konovalov, et al., Laser speckle contrast imaging in neurosurgery: a systematic review, *World Neurosurg.* 171 (2023) 35–40.
- [29] L. Engqvist, et al., Inferior rectus muscle detachment during strabismus surgery has a major effect on anterior segment perfusion, as shown by LSCI perfusion monitoring, *Br. J. Ophthalmol.* 109 (6) (2025) 704–708.
- [30] P.M. Kuri, et al., Deep learning-based image analysis for the quantification of tumor-induced angiogenesis in the 3D *In vivo* tumor model—establishment and addition to laser speckle contrast imaging (LSCI), *Cells* 11 (15) (2022) 2321.
- [31] B. Kim, et al., Measuring human cerebral blood flow and brain function with fiber-based speckle contrast optical spectroscopy system, *Commun. Biol.* 6 (1) (2023) 844.
- [32] G. Yu, Diffuse correlation spectroscopy (DCS): a diagnostic tool for assessing tissue blood flow in vascular-related diseases and therapies, *Curr. Med. Imaging* 8 (3) (2012) 194–210.
- [33] W. Zhong, et al., Efficacy of manipulative acupuncture therapy monitored by LSCI technology in patients with severe Bell’s Palsy: a randomized controlled trial, *Evid. Based Complement. Alternat. Med.* 2020 (1) (2020) 6531743.
- [34] T. Durduran, A.G. Yodh, Diffuse correlation spectroscopy for non-invasive, microvascular cerebral blood flow measurement, *Neuroimage* 85 (2014) 51–63.
- [35] C.P. Valdes, et al., Speckle contrast optical spectroscopy, a non-invasive, diffuse optical method for measuring microvascular blood flow in tissue, *Biomed. Opt. Express* 5 (8) (2014) 2769–2784.